

HYPERON POLARIZATION IN HADRONIC COLLISIONS

S. BANERJEE

Tata Institute of Fundamental Research, Homi Bhabha Road, Bombay 400 005, India.

ABSTRACT

The polarization of hyperons produced in inclusive hadronic collisions has been reviewed. The polarization seems to increase in magnitude with an increase in the transverse momentum of the hyperon almost in a linear fashion. The magnitude of the polarization of all the hyperons seems to be the same at a given transverse momentum. However the sign of the polarization differs from hyperon to hyperon viz it is positive for Σ 's and negative for Λ , Ξ 's. Λ -polarization in the target fragmentation region is weakly dependent on the c.m. energy and the beam particle. Nuclear targets yield a somewhat smaller value of the polarization which can be understood as a rescattering effect in the nucleus. The polarization measurements have been compared with the predictions of Regge pole models as well as those of quark models involving fragmentation and recombination. Polarized hyperons have provided some precise measurements of the hyperon magnetic moments. These measurements need a more refined static quark model to explain the spectroscopic properties of baryons.

1. INTRODUCTION

THE non-zero polarization of Λ 's produced in inclusive p -Be collisions¹ at 300 GeV/c at large transverse momenta and the almost linear correlation between the polarization and the transverse momentum created a lot of interest in studies of hyperon polarization in inclusive collisions. The observed polarization is along the normal to the plane of production of the hyperon, i.e. the plane containing the beam and the hyperon. This observation was confirmed with a variety of beams at different c.m. energies²⁻¹⁰ for inclusive Λ as well as other hyperons.

The study of hyperon polarization has indeed given insight to the strong interaction dynamics. In addition the polarized hyperons provide a means of determining the magnetic moments of the hyperons very accurately. These results on the magnetic moments of hyperons have been a testing ground of static quark models.

The plan of the paper is as follows: Section 2 will summarize the experimental data available on hyperon polarization. The theoretical framework to study the hyperon polarization will be

briefly outlined in §3. Section 4 will contain a comparison of the model predictions with the existing data. Measurements of hyperon magnetic moments and the implication of these measurements will be discussed in §5. The main conclusions will be summarized in §6.

2. EXPERIMENTAL DATA ON HYPERON POLARIZATION

The hyperon polarization P_z^h is measured through its decay angular distribution. From N hyperon decays, one can estimate P_z^h through

$$P_z^h = \{3/(\alpha N)\} \sum_i \hat{k}_i \cdot \hat{n}_i$$
$$\Delta P_z^h = \frac{1}{\alpha} \left[\frac{3 - (\alpha P_z^h)^2}{N} \right]^{1/2}, \quad (1)$$

where \hat{n}_i = unit vector along the direction of the z -axis; \hat{k}_i = unit vector along the decay baryon in the hyperon rest frame; and α = the analyzing power of the hyperon. The values of the analyzing powers of various hyperons are summarized in table 1.

Table 1 Analyzing powers of hyperons

Hyperon type	Decay channel	Analyzing power α
Λ	$p \pi^-$	$+0.642 \pm 0.013$
Λ	$n \pi^0$	$+0.646 \pm 0.044$
Σ^+	$p \pi^0$	-0.979 ± 0.016
Σ^+	$n \pi^+$	$+0.066 \pm 0.016$
Σ^-	$n \pi^-$	-0.068 ± 0.008
Ξ^0	$\Lambda \pi^0$	-0.413 ± 0.022
Ξ^-	$\Lambda \pi^-$	-0.434 ± 0.015

The definition of the normal to the production plane varies from one experiment to another, which results in a flip in the sign of the measured polarization. In this summary, we have tried to keep the following definition of the normal, \hat{n}

$$\hat{n} = \frac{\mathbf{k}^{\text{target}} \times \mathbf{k}^h}{|\mathbf{k}^{\text{target}} \times \mathbf{k}^h|}, \quad (2)$$

where the target (hyperon) momentum $\mathbf{k}^{\text{target}}$ (\mathbf{k}^h) is measured in the c.m. frame.

The bulk of the available data is for inclusive Λ -production. As one knows, a large fraction of the Λ 's comes from the decays of the heavier resonances and in most of the analyses, one has not taken into account of this. Now for Σ^0 decays it has been shown¹¹ that the decay Λ 's from Σ^0 has polarization $P_{\Sigma^0}^{\Lambda}$ given by

$$P_{\Sigma^0}^{\Lambda} = -P^{\Sigma^0}/3. \quad (3)$$

Even if one takes $P^{\Sigma^0} = -P^{\Lambda}$ (as has been suggested by some of the models), the observed Λ -polarization is significantly smaller than the true polarization of the directly produced Λ 's. One should remember this fact when one compares the data with the model predictions.

The data can broadly be classified into two categories depending on the nature of the target, (a) hydrogen target, (b) nuclear target. Hyperons are produced mainly through the fragmentation of the target. The mechanism of the strange quark production can cause a further classification into two categories: (i) strange quark coming from the sea. Examples of such processes are target fragmentation with π^+ , K^+ , p , \bar{p} beams and also certain final states using K^- beam



(ii) The valence strange quark from the beam takes part in the formation of the hyperon, which can only be seen in K^- -induced reactions where the final states should be



In Regge language¹² the K^- induced Λ production data have been understood in terms of ' K^+ ' exchange at the $p\bar{\Lambda}$ vertex and this implies that there will be a K^-K^+ interaction at the other vertex. It has been shown¹² that the process (5) can be identified with strangeness annihilation and it should have an energy dependence s^{-1} , whereas the process (4) is due to strangeness non-annihilation. The non-annihilation component has two components with energy dependence $s^{-1/2}$, s^0 due to normal meson and pomeron exchange. Indeed the separation of the component (4) has been done (figure 1a) and one sees that the abundance of the non-annihilation component in the inclusive Λ data increases with c.m. energy. The polarization of the Λ 's produced in the two sub-processes has been separated in a 4.2 GeV/c K^-p experiment. There one finds (figures 1b, 1c) that the Λ -polarization in the strangeness annihilation process (K_A^-) differs significantly from those in the strangeness non-annihilation process (K_{NA}^-).

2.1. Energy dependence of Λ -polarization

The Λ -polarization data in the target fragmentation region have been plotted separately for π^+ , K^+ and proton beams (figure 2a); K_{NA}^- , π^- , \bar{p} beam (figure 2b). The Λ -polarization is slightly negative and it stays almost constant over the entire energy range for π^+ , K^+ , K_{NA}^- and \bar{p} beams. On the other hand the proton beam data show a strong positive polarization at all the energy points where data are available.

For K^- beam, Λ -polarization data exist in the kaon fragmentation region as well and there (figure 2c) one sees again no or very little energy dependence over the entire energy region scanned. The value is negative but the magnitude of the polarization is somewhat larger than that observed in the proton fragmentation region with π^+ , K^+ , π^- , K_{NA}^- or \bar{p} beams.

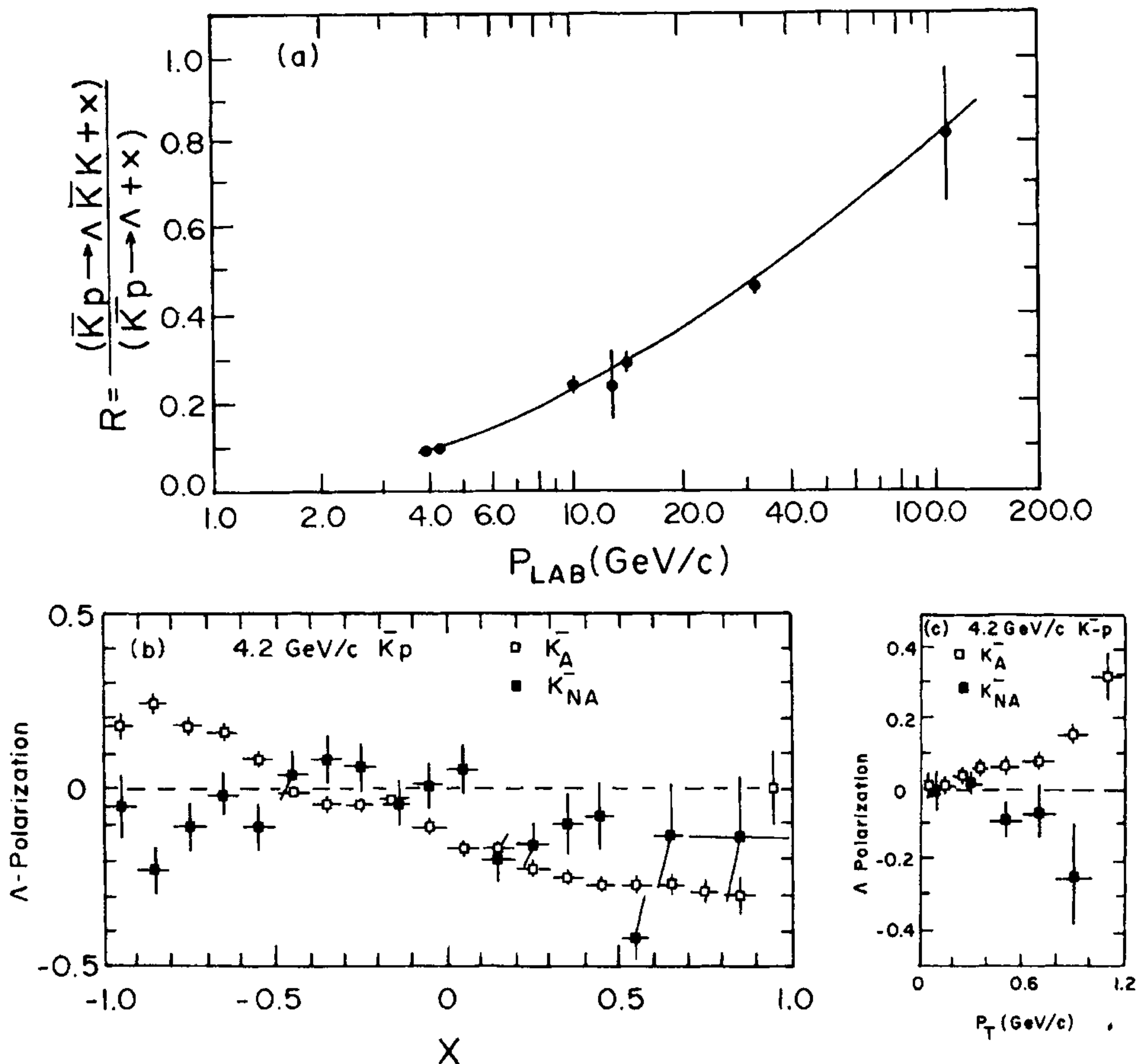


Figure 1a. The fraction of strangeness non-annihilation component in the inclusive Λ sample produced in K^-p interactions as a function of the beam momentum. **b-c.** Λ -polarization for inclusive Λ sample produced via strangeness annihilation and non-annihilation in 4.2 GeV/c K^-p interactions as a function of (b) Feynman x , (c) transverse momentum.

2.2. Dependence on kinetic variables

Figures 3a and 3b show the Λ -polarization measured as a function of the Feynman x variable for K_{NA}^- , π^- , \bar{p} induced and π^+ , K^+ , p induced processes respectively. Again the data show no energy or beam particle dependence over the entire x -region except at very large x -values in $p-p$ collisions where a large positive polariz-

ation is observed. The x -dependence is otherwise not very strong. Figure 3c shows the Λ -polarization in the kaon fragmentation region plotted as a function of x . Again no energy dependence is observed. However, there is an indication of some increase in the magnitude of the polarization with increase in x ($P^\Lambda \approx 0.0$ near $x = 0$ and $P^\Lambda \approx -0.3$ to -0.4 at $x = 1$).

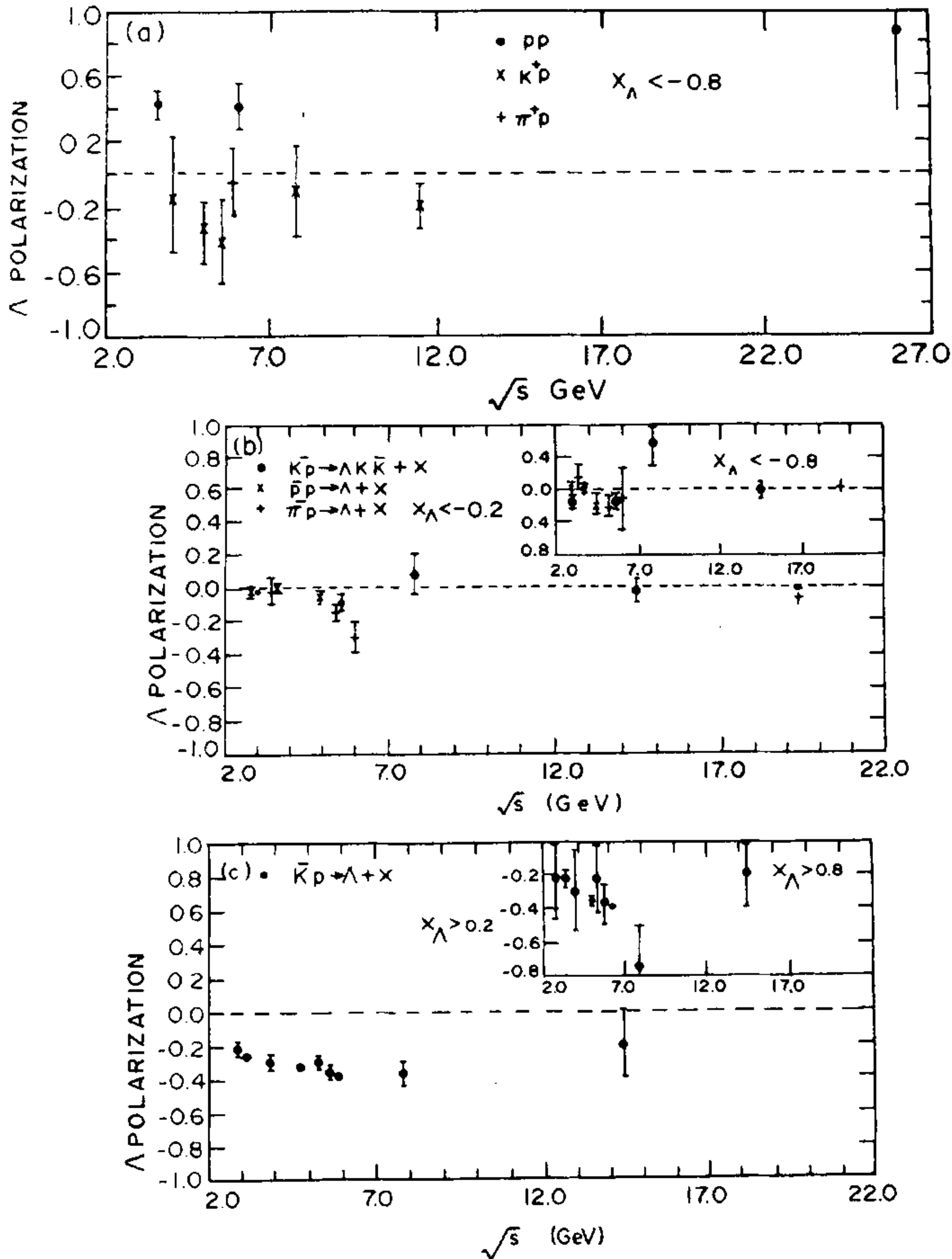


Figure 2. Λ -polarization as a function of c.m. energy in (a) proton fragmentation region with p, π^+, K^+ beams, (b) proton fragmentation region with \bar{p}, π^-, K^- beams, (c) kaon fragmentation region.

Figure 4a shows the dependence of Λ -polarization on transverse momentum p_T of Λ . As has been seen by Bunce *et al*¹, there is almost a linear dependence of Λ -polarization with its transverse momentum taking large negative values at large p_T . This phenomenon does not depend on the

beam type nor its energy. Figure 4b shows similar data for photo-production processes. Although the overall data do not show any p_T dependence, one sees large negative polarization at large p_T values in the target fragmentation region (by restricting $x_\Lambda < 0$).

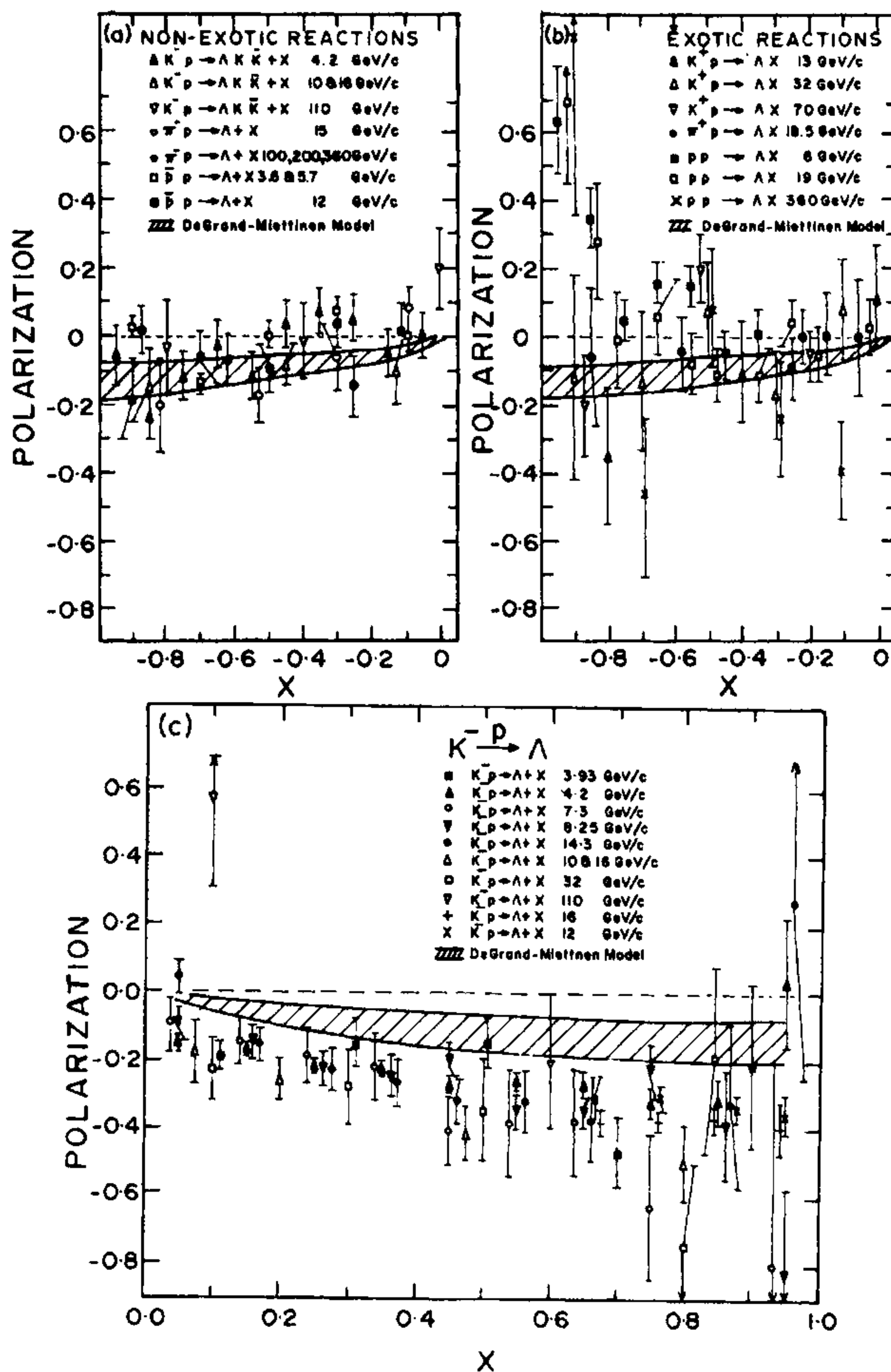


Figure 3. Λ -polarization as a function of Feynman x in (a) proton fragmentation region with p, π^+, K^+ beams, (b) proton fragmentation region with \bar{p}, π^-, K_{NA}^- beams, (c) kaon fragmentation region.

2.3. A -dependence

Figure 5a shows the Λ -polarization data as a function of p_T for hydrogen and deuterium targets (both with proton beam at 28.5 GeV/c). There is hardly any difference in the two sets of measurements and one sees the already established linear correlation between P^Λ and p_T in the

data. Figure 5b shows the polarization data on Be-target using proton beams at three different energies. These three sets cover different x -region for a given p_T value (x -range may differ by 30%). The close agreement between the three sets indicates a rather weak x -dependence of the polarization. However, when one compares the combined H-De data with the combined Be data

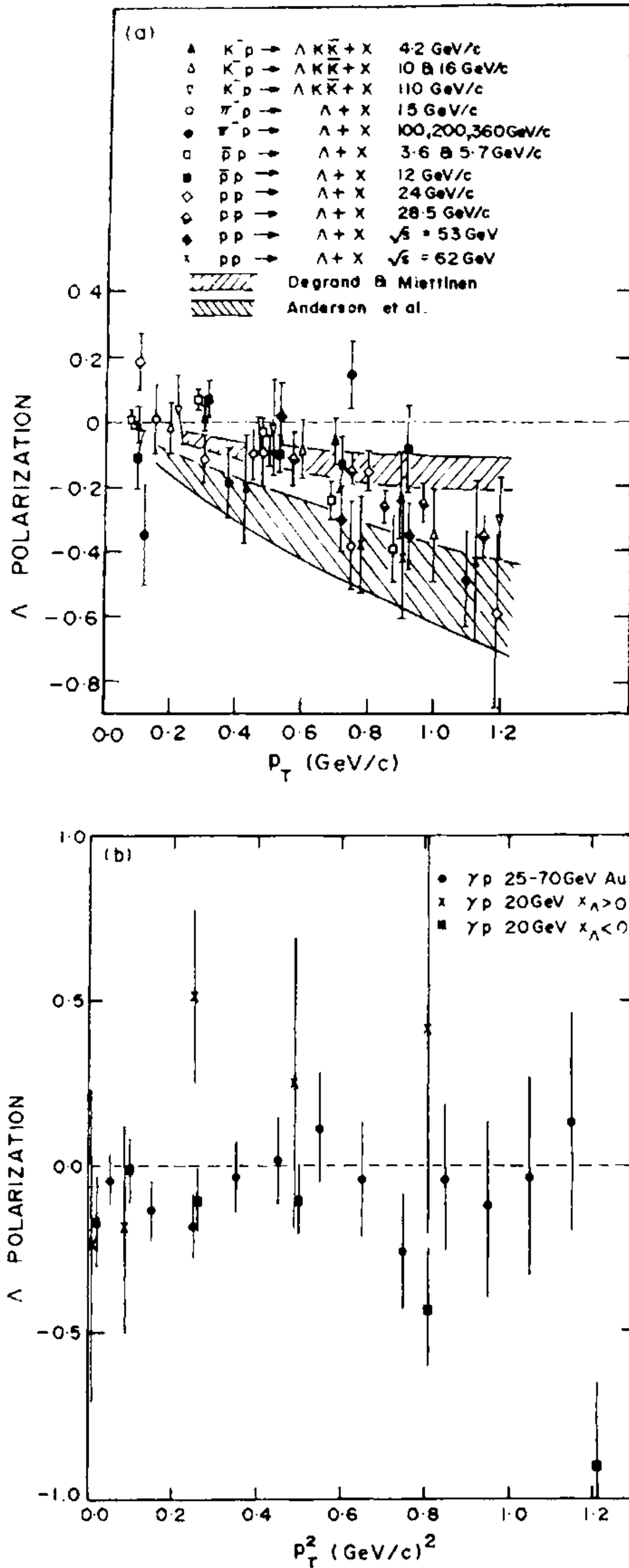


Figure 4. Λ -polarization as a function of (a) p_T in proton fragmentation region with $p, \bar{p}, \pi^\pm, K^+, K_{NA}^-$ beams (b) p_T^2 with γ beam, overall and also in the proton/photon fragmentation regions.

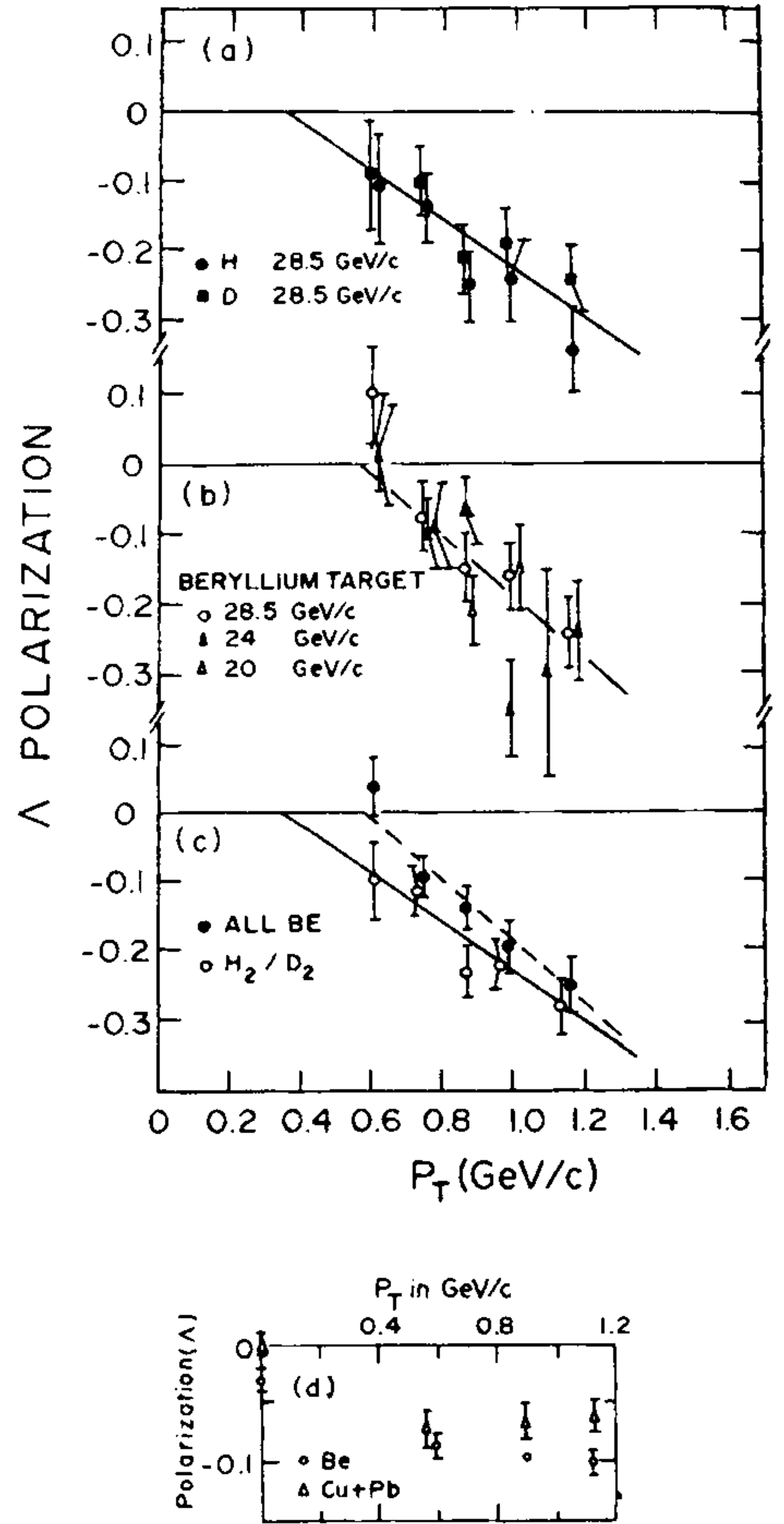


Figure 5. Λ -polarization as a function of p_T in proton-induced collisions for (a) hydrogen and deuterium targets, (b) Be target at 3 different beam momenta, (c) hydrogen/deuterium and Be targets, (d) Be and copper/lead targets.

(figure 5c), one sees that the Be-target results have somewhat smaller magnitude for P^Λ . This has been corroborated by comparing the Λ -polarization data in Be and Pb/Cu targets using 400 GeV/c proton beam (figure 5d). Thus the Λ -

polarization in nuclear targets is significantly smaller and the magnitude of the polarization decreases with increase in A-number of the target. The nuclear target may tend to wash out the polarization effects through another scatter of the Λ in the struck nucleus.

2.4. Polarization of other hyperons

Polarization data exist for Σ^+ , Σ^- , Ξ^0 , Ξ^- in proton-nucleus collisions at high energies. They all show (figures 6a,b) an approximate linear dependence of the hyperon polarization with p_T and the magnitude of the polarization gets significantly large at large p_T values. While Ξ^0 , Ξ^- are polarized in the same direction as Λ , the polarization direction is flipped in the case of Σ 's.

Polarization data exist for Ξ^- (figure 7a), Σ^0 (figure 7b) and Σ^{*+} (not shown) in K^-p collisions. The x-dependence of Ξ^- polarization is similar to that of Λ . However, the data on Σ^0 are not good enough to make a similar statement. Polarization data on $\bar{\Lambda}$ exist in pp as well as K^+p collisions (figure 7c). The $\bar{\Lambda}$'s produced in p -nucleus collisions are not polarized, whereas the $\bar{\Lambda}$'s produced in the K^+ fragmentation are significantly polarized.

3. THEORETICAL FRAMEWORK

There are basically two approaches to understand the hyperon polarization in hadronic collisions. The old approach is to use the Regge pole exchange ideas¹³. In the other method, one tries to understand the hyperon polarization through quark fragmentation or quark recombination models¹⁴⁻¹⁶.

3.1. Regge pole approach

Single and triple Regge¹³ analyses for the unpolarized cross sections have been extended to explain the polarization measurements. In fact the polarization measurements can give rise to information on the Regge exchanges which are not accessible to the unpolarized cross-sections. For the inclusive process,

$$a + b \rightarrow c + X, \quad (6)$$

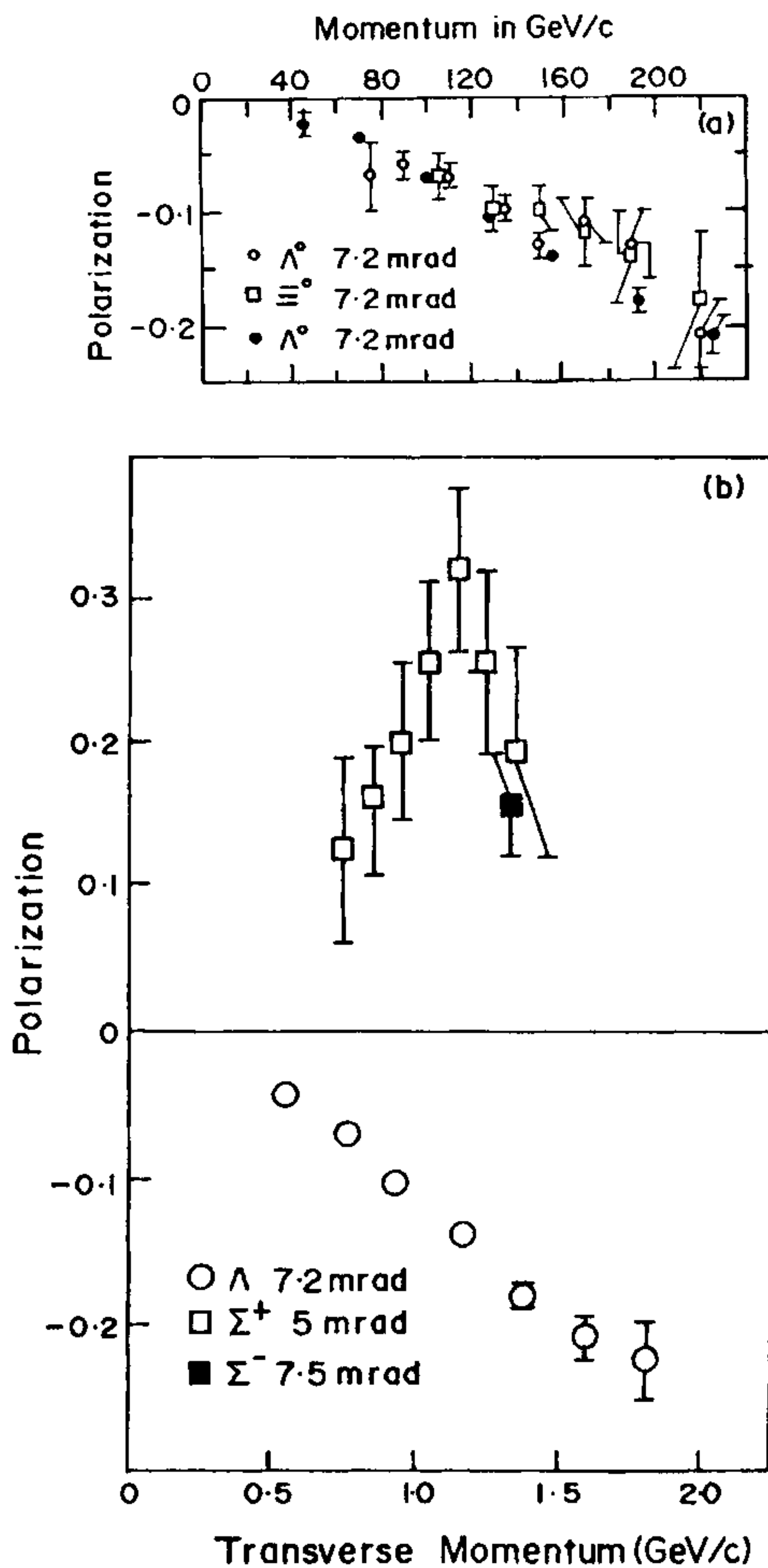


Figure 6(a). Λ and Ξ polarization measurements in proton-nucleus collisions at a fixed production angle as a function of the hyperon momentum. **(b)** Λ , Σ^+ and Σ^- polarization measurements in proton-nucleus collisions as a function of transverse momentum.

let us examine the polarization at the fragmentation vertex, i.e. $b \rightarrow c$. There are three distinct classes for Λ -polarization. (a) Exotic processes ($ab\bar{c}$ exotic and $b\bar{c}$ non-exotic): The polarization should be independent of energy and also of the

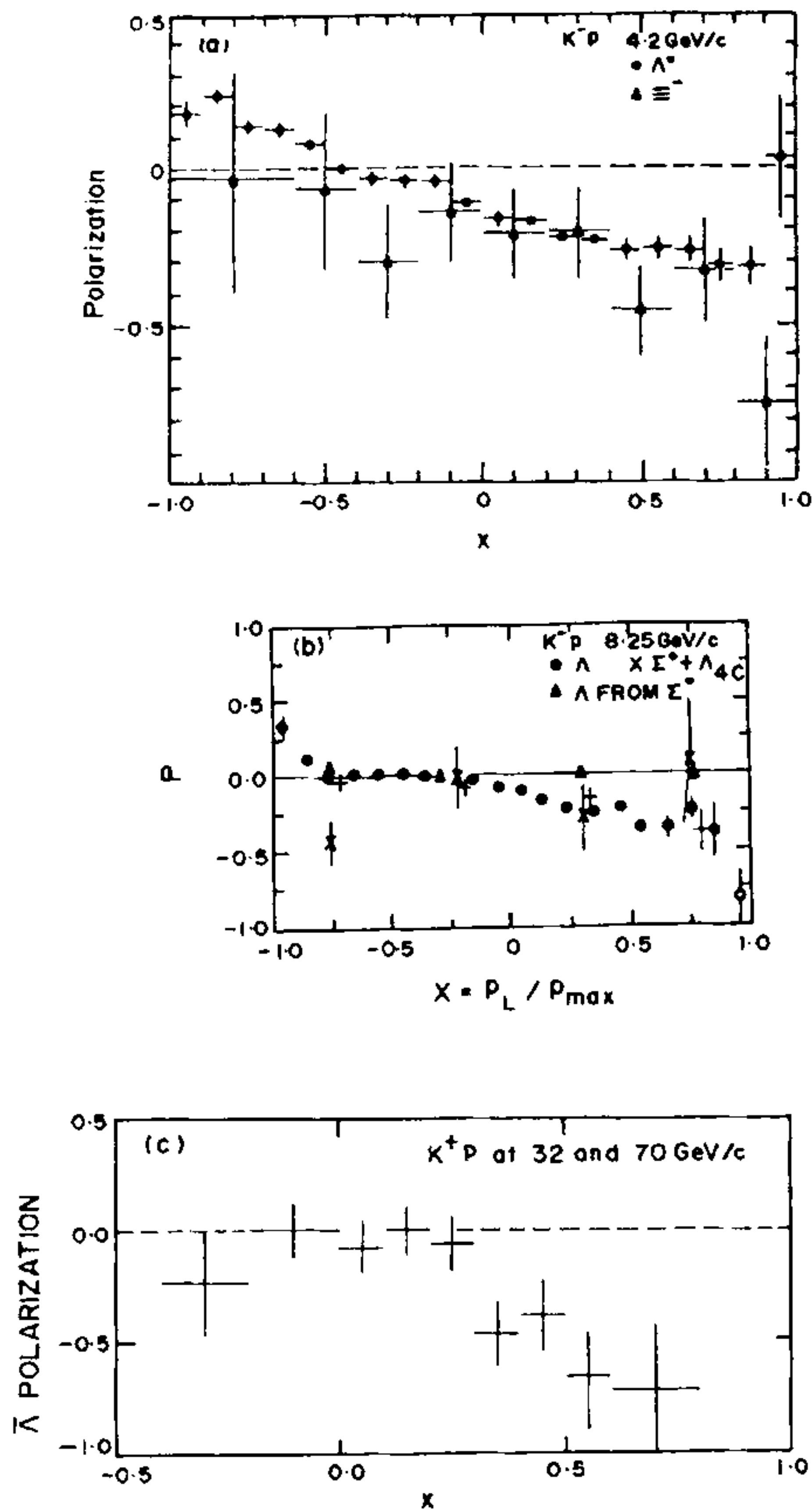


Figure 7(a). Λ and Ξ^- polarization in K^-p interactions at 4.2 GeV/c as a function of Feynman x. **(b).** Λ , Σ^0 , Λ_{4C} (in 4C fits), Λ_Σ (from Σ^0 decay) polarization as a function of Feynman x in K^-p interactions at 8.25 GeV/c. **(c).** $\bar{\Lambda}$ polarization in K^+p interactions at 32 and 70 GeV/c as a function of Feynman x.

incident particle a . Examples of such processes are $p \xrightarrow{p, K^+, \pi^+} \Lambda$. (b) Non-exotic processes (abc and $b\bar{c}$ non-exotic): At a given energy, the polarization is expected to be independent of a for a set of non-exotic reactions where the relative

Reggeon to Pomeron contributions are expected to be approximately equal by the exchange degeneracy and the two-body coupling constants. Examples for such processes are $p \xrightarrow{\pi^-, K_{NA}^-, \bar{p}} \Lambda$. Using f -Pomeron proportionality as a crude approximation, one expects the above nonexotic processes to be roughly energy-independent. (c) Strangeness annihilation: The annihilation components $p \xrightarrow{K_A^-} \Lambda$ is also expected to have energy-independent polarization.

Detailed prediction on hyperon polarization is, however, limited, since the polarized as well as the unpolarized cross-sections involve complicated residue functions which are input to the model.

3.2. Quark model approach

In the quark models, the hyperon polarization stems from the production mechanism of the strange quark which forms the valence partner in the hyperon. Let us consider the hyperon Λ . It is made of uds quarks of which ud make a diquark state of $I = J = 0$. Thus the hyperon spin is the same as the strange quark spin and hence the polarization. In the literature, there are basically three approaches: (1) Lund model¹⁴ using fragmentation of quarks (2, 3) models due to DeGrand-Miettinen¹⁵ and Szwed¹⁶ using quark recombination. It is clear that, in these models, the polarization of the hyperon from $p \xrightarrow{a} h$ will be independent of the incident particle a as long as the production mechanism of the s -quark remains the same. This is more or less true for $a = \pi^\pm, p, \bar{p}, K^+$ and K_{NA}^- where the s -quark comes from the sea, whereas $a = K_A^-$ uses a distinctive different mechanism.

3.2a. Lund model

In this approach, a linear colour field is stretched and the fragmentation process proceeds by producing a $q\bar{q}$ pair which breaks the colour field. If the $q\bar{q}$ pair is massless, the pair can be classically produced in a single spacetime point and afterwards pulled apart by the colour force field. However, if the quark has a transverse

mass (mass and/or transverse momentum), the situation cannot occur classically if the energy-momentum is to be conserved. Thus the quark and the anti-quark are produced at a distance so that the energy of the force field in between them can be transformed into the transverse mass. This will create an orbital angular momentum perpendicular to the string. The angular momentum conservation thus demands that the $q\bar{q}$ pair will be polarized so that the spin of the pair compensates the orbital angular momentum.

Let us consider Λ production with a definite value of transverse momentum \mathbf{p}_T . There will be an enhanced number of events where \mathbf{k}_T (the transverse momentum of the s -quark) points in the same direction as \mathbf{p}_T . The correlation of \mathbf{k}_T and the spin of the s -quark will make the Λ 's polarized. This is a so-called trigger bias effect. Similarly one can predict polarization of the other hyperons in this model. Detailed consideration gives that Σ 's would have positive polarization, whereas Λ , Ξ 's would have negative polarization as borne out by the data.

3.2b. Recombination model

In this model, proton in the infinite momentum frame is built up of three valence quarks and a large number of sea partons. In the collision, the slow or 'wee' partons interact destroying the coherence of the wave function. The parton-to-hadron transformation takes place semilocally in rapidity and is pictured as proceeding via quark recombinations. The fastest particles are formed by the recombination of the beam's valence quarks with other valence or sea quarks. Baryons can be formed via recombination of two valence quarks with a sea quark (VVS , e.g. Λ , Σ^+ , Σ^0) or via recombination of one valence quark with two sea quarks (VSS , e.g. Σ^- , Ξ^0 , Ξ^-). Here all baryons are described by nominal $SU(6)$ wave functions. One assumes all sea quarks to be initially polarized and the recombination mechanism enhances asymmetry in one spin state over the other. Baryons are treated as a bound state of quark and a diquark where the diquark is made of two most similar quarks (i.e. 2 valence quarks in VVS and 2 sea quarks in VSS). With the

following three assumptions, one can then relate the polarization of various hyperons in different fragmentation processes. (1) The effect of recombination on the partons as they are transferred to the outgoing hadron may be different depending on whether they are accelerated (sea partons) or decelerated (valence partons). (2) Two partons with similar wave functions (VV or SS) may interact with themselves differently than they interact with a parton of dissimilar wave function (VS). (3) The transverse momenta of the outgoing hadron and its constituents are more or less parallel (i.e. recombination is short range in p_T).

In terms of ϵ , δ , the asymmetries a quark and diquark recombination amplitudes, the polarization of various hyperons can be summarized as given in table 2.

In the DeGrand-Miettinen model, one considers the effect of the non-colinear boost in the recombination process. The s -quark resides in the sea and carries a small fraction ($x_x \sim 0.1$) of the momentum whereas it is a valence quark of Λ and carries a large fraction ($\sim 1/3$) of the Λ 's momentum. Since Λ carries a large fraction x_F of the proton's momentum, the recombination process boosts the longitudinal momentum of the s -quark from $x_s p$ to $x_F p/3$. The s -quark also carries transverse momentum; on average it is the same in proton as well as in Λ . The velocity vector of the s -quark is thus not parallel to the direction of the change in momentum induced by the recombination process. This will result in a boost and a rotation and hence an additional spin-dependant component will appear in the Hamiltonian. This will give rise to the polarization asymmetry similar to Thomas precession in atomic physics.

Table 2 Polarization of hyperon

Channel	Polarization	Recombination
$p \rightarrow \Lambda$	$-\epsilon$	VVS
$p \rightarrow \Sigma^+/\Sigma^0$	$(\epsilon + 2\delta)/3$	VVS
$p \rightarrow \Sigma^-$	$(4\epsilon - \delta)/6$	VSS
$p \rightarrow \Xi/\Xi^0$	$-(\epsilon + 2\delta)/3$	VSS
$\pi/K^+ \rightarrow \Lambda$	$-\delta/2$	VSS
$K^- \rightarrow \Lambda$	ϵ	VSS
$p \rightarrow \bar{\Lambda}$	0	SSS
$\gamma \rightarrow \Lambda$	$-\delta/2$	

In the Szwed model, one assumes that the large p_T hyperons will preferentially have large p_T partons and the transverse momentum of the sea partons is generated through its multiple collisions in the quark-gluon matter. For a sea quark with non-zero mass, this process will make the quark polarized. This is of course a nonperturbative calculation and hence no quantitative prediction can be made in this model for low p_T processes.

4. COMPARISON OF THE DATA WITH THE MODEL PREDICTIONS

One sees that the polarization of Λ in the proton fragmentation region is almost energy-independent (figures 2a, b). They are also independent of beam for π^\pm , K^+ , K_{NA}^- , \bar{p} (see table 3).

This is expected from the triple Regge model as well as from the quark model. However the polarization with proton beam is significantly different from those with other beams. Polarization in the kaon fragmentation region is also energy-independent as expected in the Regge pole model. However, the magnitude of the polarization of the polarization is significantly larger in the kaon fragmentation region than in the proton fragmentation region with K_{NA}^- , π^- , \bar{p} , K^+ , π^+ beams. This is in contradiction with the recombination model predictions.

Table 3 Λ polarization for various beams

$P(p \rightarrow \Lambda)$			
$a = K_{NA}^-, \pi^-, p^-$	$a = K^+, \pi^+$	$a = p$	$P(K^- \rightarrow \Lambda)$
-0.06 ± 0.05	-0.14 ± 0.11	$+0.41 \pm 0.07$	-0.30 ± 0.01

x -dependence of the polarization is explicitly given in the model of DeGrand-Miettinen. The polarization is largely x -independent in the proton as well as in the kaon fragmentation regions (figures 3a-c). The hatched regions in these figures are due to the model prediction and agree with the data except in the case of $p \rightarrow \Lambda$ at large x_F values which shows large positive polarization.

The p_T dependence of Λ -polarization in the proton fragmentation region (figure 4a) shows almost linear increase with p_T . Both Lund model and DeGrand-Miettinen model predict similar behaviour (shown by the hatched regions in the figure). The gross feature of the data is explained by both the models. However, the Λ -polarization in the kaon fragmentation region seems somewhat larger as shown in table 4, where the data at different energies have been combined in 3 different p_T regions.

The Σ^+ , Σ^- polarizations are found to be positive and of the same magnitude as of Λ -polarization. The Ξ^0 , Ξ^- polarizations have the same sign as well as magnitude as of Λ -polarization. These are in agreement with the quark model predictions.

5. MAGNETIC MOMENT MEASUREMENTS

The observation that the hyperons are polarized in hadronic collisions at large p_T has led to some precise measurements of the hyperon magnetic moments. In a typical experiment¹⁷ to measure Σ^+ magnetic moment, a beam of protons is incident on a copper target at an angle with respect to the horizontal plane. The target was placed at an upstream end of a magnet and a secondary beam emerging from the magnet was limited by a tungsten channel to a very narrow emittance. The hyperons produced decay in a

Table 4 p_T dependence of Λ polarization

p_T (GeV/c)	$P(p \xrightarrow{K_{NA}^-} \Lambda)$	$P(p \xrightarrow{\bar{p}} \Lambda)$	$P(p \xrightarrow{p} \Lambda)$	$P(K^- \rightarrow \Lambda)$
0.0 - 0.4	$+0.01 \pm 0.03$	$+0.04 \pm 0.02$	$+0.01 \pm 0.04$	-0.12 ± 0.01
0.4 - 0.8	-0.07 ± 0.04	-0.07 ± 0.02	-0.10 ± 0.02	-0.25 ± 0.01
0.8 - 1.2	-0.29 ± 0.08	-0.16 ± 0.08	-0.30 ± 0.03	-0.44 ± 0.02

Table 5 Magnetic moments for hyperons

Hyperon	Experimental measurement (μ_N)	Naive quark model prediction (μ_N)
Λ	-0.6138 ± 0.0047	-0.58
Σ^+	$+2.355 \pm 0.016$	+2.68
Σ^-	-0.89 ± 0.14	-1.05
Ξ^0	-1.253 ± 0.014	-1.40
Ξ^-	-0.69 ± 0.04	-0.47

decay region and there are downstream counters to detect and analyze the decay products. The Σ^+ 's produced with a polarization will precess in the magnetic field and this would modify the decay angular distribution. The fit to the decay angular distribution measures the angle of precession and hence the magnetic moment of the hyperon.

The magnetic moments for all the hyperons^{17, 18} (measured so far) are summarized in table 5. For comparison, the predictions of a naive quark model¹⁹ are also given in the table. The quark model assumes that the baryon $\frac{1}{2}^+$ octet has an *S*-wave colour singlet structure. The overall agreement is qualitatively good. However, there are substantial differences in the absolute values ($\sim 0.2-0.3 \mu_N$) compared to the experimental uncertainties. A non-relativistic static quark model is thus inadequate and one has to incorporate orbital effects, exchange current etc. No single model has emerged so far which will explain all the magnetic moments successfully. Quark anomalous magnetic moments have to be incorporated.

6. SUMMARY

(i) Λ -polarization is consistent with no dependence on incident beam momentum in proton as well as kaon fragmentation region in agreement with model predictions.

(ii) Λ -polarization in the target fragmentation region for K^+ , π^+ , K_{NA}^- , π^- , \bar{p} hardly depends on the beam particle and has very weak x -dependence in agreement with the quark model picture. However, proton beam data show a large

positive polarization in the region $-1.0 < x < -0.8$ which cannot be accounted for in any of the models.

(iii) Λ -polarization in the kaon fragmentation region is large and increases with x while it is small and nearly independent of x in the proton fragmentation region (except for the point mentioned in (ii) above). This is in disagreement with the quark model prediction due to DeGrand-Miettinen.

(iv) Λ -polarization increases linearly with p_T in the proton as well as in the kaon fragmentation region. The p_T dependence is well explained by the quark models.

(v) Polarization effect is reduced in nuclear targets which can be qualitatively understood by the rescatter effect inside the nucleus.

(vi) Polarization data for Σ 's show positive values whereas those for Ξ 's show negative values (like Λ). The polarization increases almost linearly with p_T and the correlation of polarizations of the various hyperons can be understood in the framework of quark models.

(vii) Hyperon polarization has led to very precise measurements of hyperon magnetic moments. These measurements demand a more refined static quark model to explain the baryon spectroscopy.

29 March 1986

1. Bunce, G. *et al.*, *Phys. Rev. Lett.*, 1976, **36**, 1113.
2. Λ -polarization data in $\pi^\pm p$ collisions: Sugahara, R. *et al.*, *Nucl. Phys.*, 1979, **B156**, 237; Barreiro, F. *et al.*, *Phys. Rev.*, 1978, **D17**, 669; Besinger, J. *et al.*, *Phys. Rev. Lett.*, 1983, **50**, 313; Stutenbeck, P. H. *et al.*, *Phys. Rev.*, 1974, **D9**, 608; Biswas, N. N. *et al.*, *Nucl. Phys.*, 1980, **B167**, 41.
3. Λ -polarization data in $K^\pm p$ collisions: Chliapnikov, P. V. *et al.*, *Nucl. Phys.*, 1976, **B112**, 1; Barletta, W. *et al.*, *Nucl. Phys.*, 1973, **B51**, 499; Faccinni-Turluer, M. L. *et al.*, *Z. Physik.*, 1979, **C1**, 19; Barth, M. *et al.*, *Z. Physik.*, 1981, **C10**, 205; Borg, A. *et al.*, *Nuovo Cimento*, 1974, **A22**, 559; Ganguli, S. *et al.*, *Nuovo Cimento*, 1978, **A44**, 345; Ganguli, S. *et al.*, *Nucl. Phys.*, 1977, **B128**, 408; Chung, S. U. *et al.*, *Phys. Rev.*, 1975, **D11**, 1010; Baubillier, M. *et al.*, *Nucl. Phys.*, 1979, **B148**, 18; Grassler, H. *et al.*, *Nucl. Phys.*, 1978, **B136**, 386.

- Abramowicz, H. *et al.*, *Nucl. Phys.*, 1976, **B105**, 222; Armstrong, T. *et al.*, *Nucl. Phys.*, 1980, **B173**, 154; Haupt, T. *et al.*, *Z. Physik.*, 1985, **C28**, 57.
4. Λ $\bar{\Lambda}$ -polarization data in $\bar{p}p$ collisions: Banerjee, S. *et al.*, *Nucl. Phys.*, 1979, **B150**, 119; Ganguli, S. *et al.*, *Nucl. Phys.*, 1973, **B53**, 458; Bertrand, D. *et al.*, *Nucl. Phys.*, 1977, **B128**, 365.
 5. Λ -polarization data in γp collisions: Abe, K. *et al.*, *Phys. Rev.*, 1984, **D29**, 1877; Aston, D. *et al.*, *Nucl. Phys.*, 1982, **B195**, 189.
 6. Λ -polarization data in pp collisions: Lesnik, A., *et al.*, *Phys. Rev. Lett.*, 1975, **35**, 770; Aahlin, P. *et al.*, *Nuovo Cimento Lett.*, 1978, **21**, 236; Blobel, V. *et al.*, *Nucl. Phys.*, 1977, **B122**, 429; Asai, M. *et al.*, *Z. Physik.* 1985, **C27**, 11.
 7. Λ -polarization data in p -nucleus collision: Heller, K. *et al.*, *Phys. Rev. Lett.*, 1978, **41**, 607; Heller, K. *et al.*, *Phys. Lett.*, 1977, **B68**, 480; Heller, K. *et al.*, *Phys. Rev. Lett.*, 1980, **45**, 1043; Heller, K. *et al.*, *Phys. Rev. Lett.*, 1980, **51**, 2025; Raychaudhuri, K. *et al.*, *Phys. Lett.*, 1980, **B90**, 319; Lomano, F. *et al.*, *Phys. Rev. Lett.*, 1980, **43**, 1905 (see also 1).
 8. $\bar{\Lambda}$ -polarization in $K^\pm p$, γp and p -nucleus collisions: Chliapnikov, P. V. *et al.*, *Nucl. Phys.*, 1976, **B112**, 1; Barletta, W. *et al.*, *Nucl. Phys.*, 1973, **B51**, 499; Faccinni-Turluer, M. L. *et al.*, *Z. Physik.*, 1979, **C1**, 19; Ajienenko, I. V. *et al.*, *Phys. Lett.*, 1983, **B121**, 183; Barth, M. *et al.*, *Z. Physik.*, 1981, **C10**, 205; Aston, D. *et al.*, *Nucl. Phys.*, 1982, **B195**, 189; Heller, K. *et al.*, *Phys. Rev. Lett.*, 1978, **41**, 607.
 9. Σ^\pm , Ξ -polarization in p -nucleus collisions: Wilkenson, C. *et al.*, *Phys. Rev. Lett.*, 1981, **46**, 803; Deck, L. *et al.*, *Phys. Rev.*, 1983, **D28**, 1; Heller, K. *et al.*, *Phys. Rev. Lett.*, 1983, **51**, 2025.
 10. $\Sigma^0/\Xi/\Sigma^*$ -polarization in $K^- p$ collisions: Baubillier, M. *et al.*, *Nucl. Phys.*, 1979, **B148**, 18; Ganguli, S. *et al.*, *Nucl. Phys.*, 1977, **B128**, 408; Barreiro, F. *et al.*, *Nucl. Phys.*, 1977, **B126**, 319; Bardadin-Otwinowska, M. *et al.*, *Nucl. Phys.*, 1975, **B98**, 418.
 11. Gatto, R., *Phys. Rev.*, 1958, **109**, 610.
 12. Inami, T. *et al.*, *Phys. Lett.*, 1974, **B49**, 67.
 13. Ganguli, S. and Roy, D. P., *Phys. Rep.*, 1980, **67**, 202 (and references therein).
 14. Andersson, B. *et al.*, *Nucl. Phys.*, 1981, **B178**, 242; Andersson, B. *et al.*, *Phys. Lett.*, 1979, **B85**, 417; Andersson, B. *et al.* Lund preprint LU TP 82-4; Andersson, B. *et al.* Lund preprint LU TP 82-13.
 15. DeGrand, T. *et al.*, *Phys. Rev.*, 1981, **D23**, 1227; DeGrand, T. *et al.*, *Phys. Rev.*, 1981, **D24**, 2419; DeGrand, T. *et al.*, *Phys. Rev.*, 1985, **D31**, 661; DeGrand, T. *et al.*, *Phys. Rev.*, 1985, **D32**, 2445.
 16. Szwed, J., *Phys. Lett.*, 1981, **B105**, 403.
 17. Ankenbrandt, C. *et al.*, *Phys. Rev. Lett.*, 1983, **51**, 863.
 18. Schachinger, L. *et al.*, *Phys. Rev. Lett.*, 1978, **41**, 1348; Handler, R. *et al.*, *H. E. Spin Phys.*, 1982, (AIP, New York, 1983); Deck, L. *et al.*, *Phys. Rev.*, 1983, **D28**, 1; Cox, P. T. *et al.*, *Phys. Rev. Lett.*, 1981, **46**, 877; Rameika, R. *et al.*, *Phys. Rev. Lett.*, 1984, **52**, 581.
 19. Rosner, J. L., *High Energy Physics*, 1980, **540** (AIP, New York, 1981).

ANNOUNCEMENT

INTERNATIONAL WORKSHOP ON HOMOGENEOUS CATALYSIS—ACTIVATION OF MOLECULAR OXYGEN AND CATALYZED OXIDATIONS BY DIOXYGEN COMPLEXES

The Workshop is organized by the Central Salt and Marine Chemicals Research Institute, Bhavnagar (CSMCRI). The Workshop will be held at Bhavnagar during 3–6 October 1986. The main topics are: Novel dioxygen complexes of metal ions: synthesis, structure, equilibrium studies, kinetics of metal-dioxygen complexes formation; Oxidations catalyzed by metal-

dioxygen complexes; Oxidations catalyzed by metal-peroxo and metal-oxo complexes.

Further particulars may be had from: Prof. M. M. Taqui Khan, Chairman, Organizing Committee, International Workshop on Homogeneous Catalysis, Central Salt and Marine Chemicals Research Institute, Bhavnagar 364 002.